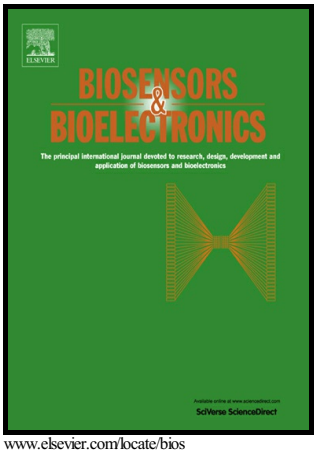

www.elsevier.com/locate/bios

Non-enzymatic Electrochemical Biosensor Based on Pt NPs/RGO-CS-Fc Nano-hybrids for the Detection of Hydrogen Peroxide in Living Cells

Zhihao Bai, Guiyin Li, Jingtao Liang, Jing Su, Yue Zhang, Huaizhou Chen, Yong Huang, Weiguo Sui, Yongxiang Zhao

PII: S0956-5663(16)30278-0
DOI: http://dx.doi.org/10.1016/j.bios.2016.04.004
Reference: BIOS8591

To appear in: *Biosensors and Bioelectronic*

Received date: 21 February 2016
Revised date: 2 April 2016
Accepted date: 4 April 2016

Cite this article as: Zhihao Bai, Guiyin Li, Jingtao Liang, Jing Su, Yue Zhang Huaizhou Chen, Yong Huang, Weiguo Sui and Yongxiang Zhao, Non-enzymatic Electrochemical Biosensor Based on Pt NPs/RGO-CS-Fc Nano-hybrids for th Detection of Hydrogen Peroxide in Living Cells, *Biosensors and Bioelectronic* http://dx.doi.org/10.1016/j.bios.2016.04.004

Non-enzymatic Electrochemical Biosensor Based on Pt NPs/RGO-CS-Fc Nano-hybrids for the Detection of Hydrogen Peroxide in Living Cells

Zhihao Bai[a,1], Guiyin Li[a,c,1], Jingtao Liang[a], Jing Su[c], Yue Zhang[b], Huaizhou Chen[b], Yong Huang[a,c*], Weiguo Sui[b*], Yongxiang Zhao[c*]

[a]School of Life and Environment Sciences, Guilin University of Electronic Technology, Guilin, Guangxi 541004, China

[b]Guangxi Key Laboratory of Metabolic Diseases Research, Guilin 181st Hospital, Guilin, Guangxi 541002, China

[c]National Center for International Research of Biological Targeting Diagnosis and Therapy, Guangxi Key Laboratory of Biological Targeting Diagnosis and Therapy Research, Collaborative Innovation Center for Targeting Tumor Diagnosis and Therapy, Nanning, Guangxi 530021, China

huangyong503@126.com

suiwg@163.com

yongxiang_zhao@126.com

*Corresponding author: Yong Huang, Ph.D., Professor, School of Life and Environment Sciences, Guilin University of Electronic Technology, Guilin, Guangxi 541004, China, Tel: (86) 773-2293135 fax: (86) 773-2293135

*Weiguo Sui, Professor: Guangxi Key Laboratory of Metabolic Diseases Research, Guilin 181st Hospital, Guilin, Guangxi 541002, China, Tel: (86) 773-2080817 fax: (86) 773-3895583

[1]These authors contributed equally to this work.

*Yongxiang Zhao, Ph.D., M.D., Professor: National Center for International Research of Biological Targeting Diagnosis and Therapy / Guangxi Key Laboratory of Biological Targeting Diagnosis and Therapy Research / Collaborative Innovation Center for Targeting Tumor Diagnosis and Therapy, Guangxi Medical University, Nanning, Guangxi 530021, China, Tel: (86) 771-5317061 fax: (86) 771-5317061.

Abstract

A highly sensitive non-enzymatic electrochemical sensor based on platinum nanoparticles/reduced graphene oxide-chitosan-ferrocene carboxylic acid nano-hybrids (Pt NPs/RGO-CS-Fc biosensor) was developed for the measurement of hydrogen peroxide (H_2O_2). The RGO-CS-Fc nano-hybrids was prepared and characterized by UV-vis spectrum, Fourier transform infrared spectroscopy, transmission electron microscopy, Raman spectrometer and electrochemical impedance spectroscopy. Under optimal experimental conditions, the Pt NPs/RGO-CS-Fc biosensor showed outstanding catalytic activity toward H_2O_2 reduction. The current response of the biosensor presented a linear relationship with H_2O_2 concentration from 2.0×10^{-8} M to 3.0×10^{-6} M with a correlation coefficient of R^2=0.9968 and with logarithm of H_2O_2 concentration from 6.0×10^{-6} M to 1.0×10^{-2} M with a correlation coefficient of R^2=0.9887, the low detection limit of 20 nM was obtained at the signal/noise (S/N) ratio of 3. Moreover, the Pt NPs/RGO-CS-Fc biosensor exhibited excellent anti-interference capability and reproducibility for the detection of H_2O_2. The biosensor was also successfully applied for the detection of H_2O_2 from living cells containing normal and cancer cells. All these results prove that the Pt NPs/RGO-CS-Fc biosensor has the potential application in clinical diagnostics to evaluate oxidative stress of different living cells.

Keywords

Non-enzymatic sensor, Graphene, Hydrogen peroxide, Ferrocene carboxylic acid, Platinum nanoparticles

Introduction

Reactive oxygen species (ROS) is deemed to be the important intracellular signaling molecules which can regulate protein synthesis, DNA damage, cell apoptosis, and other living activities. It also participates in several physiology events such as signal transition and immunity activity (Chang et al., 2013; Zhang et al., 2014). However, accumulation of excess of ROS in cells result in sabotage of intracellular activity and generate oxidative stress which is considered as the root in diseases and caducity, giving rise to damaging the balance of normal cells and tissues (Wu et al., 2011; Le et al., 2015; Khodade et al., 2014). Hydrogen peroxide (H_2O_2) is the most common representative of ROS studied in cellular environments since H_2O_2 can access and distribute into cellular compartments for long lifetime to induce various harmful biological modifications (Borgmann, 2009). However, the concentration of H_2O_2 is rather low under normal physiological and can increase to $\sim 10^{-3}$ M under pathological conditions such as traumatic brain injury ischemia-reperfusion, environmental stresses, and so on (Luo et al., 2009; Yu et al., 2015) .

Therefore, the accurate detection of H_2O_2 in cells and measurements of its dynamic release process from living cells are important to clarify the mechanism of regulating signal transduction pathways and further exploit the potential application in clinical pathological diagnosis. So far, many techniques have been developed for the determination of H_2O_2, including colorimetry（Chen et al., 2014; Lin et al., 2015), florescence（Wen et al., 2011; Shi et al., 2014), chromatography (Gimeno et al.,

2015), chemiluminescence (Yu et al., 2016), electrochemistry (Ma et al., 2015; Li et al., 2012; Chakraborty and Raj, 2009), and so on. Among these strategies, electrochemical techniques, especially the enzyme-based sensors, have been developed for the monitoring of H_2O_2 due to their high sensitivity and excellent selectivity. However, natural enzymes are sensitive to the environmental conditions and the instability of enzyme-based biosensors is inevitable.

Over the past few decades, great attention has been paid to the development of non-enzymatic electrochemical sensors because of their simplicity, high reliability, sensitivity, low cost and detect under the condition of without enzyme directly (Bianchi et al., 2014; Chen et al., 2010). In general, non-enzymatic sensor uses catalytic activity materials to catalyze related substrates and carries on the qualitative and quantitative detection of sensing device (Lee and Perk, 2010). Various nanomaterial, for example, metals (Chen et al., 2015; Qin et al., 2015), metal oxide (Lu et al., 2015) and carbon materials (Zhang et al., 2013; Sahin, 2015) had been used to fabricate non-enzymatic sensors due to their high surface reactivity, efficient charge transfer and excellent catalytic performances.

It is well known that noble metals exhibit outstanding electrocatalytic activity toward H_2O_2 redox reactions (Han et al., 2015). Particularly, Pt nanoparticles (Pt NPs) have been widely used as an excellent electrocatalyst for the detection of H_2O_2 since the presence of Pt NPs is able to trigger a strong electrocatalytic current for the evolution of hydrogen peroxide and lower the H_2O_2 oxidation/reduction overvoltage efficiently, which can easily avoid the anodic interferents like AA, UA (Chen et al., 2010). Moreover, some methods which decorating Pt NPs onto a second nanomaterials, such as Au, graphene, and so on, had been reported to improve the electrocatalytic activity and provide more active site for the anchoring of substrate in

recent years (Le et al., 2015; Zhang et al., 2014; Dey et al. 2010).

Graphene, a novel two-dimensional graphitic carbon system, have attracted enormous attention in non-enzymatic sensor because of its large specific surface area, fast heterogeneous electron-transfer rate at the graphene sheet edges, and good biocompatibility (Xiong et al., 2014; Zhang et al., 2015). Especially, reduced graphene oxide (RGO), composited through the reduction of graphene oxide, has some functional groups such as carboxyl (-COOH) and hydroxyl (-OH) groups giving rise to the better conductivity (Liu et al., 2014). It is widely used in electrochemical catalysis of H_2O_2. However, due to the strong π-π stacking among the molecular, RGO would easily generate the reunion and interlayer, which will affect the dispersion and hinder the further applications (Wang et al., 2015). Recently, surface modification of RGO by coating of chitosan have gained increasing interest due to not only the better tenability of particle size, shape and high specific surface area for large loading of guest molecules, but also assisting the dispersion of RGO in aqueous solution (Qiu et al., 2011).

Ferrocene and its derivatives, a type of organometallic chemical compound consisting of two cyclopentadienyl rings bound on opposite sides of a central ferrum atom, are widely used to construct an electrochemical biosensor as electrochemical active tag for the assay of bio-molecules (Shen et al., 2015). In our previous work, we had successfully developed an electrochemical genotyping technique via gap ligation reaction and surface hybridization detection using ferrocene carboxylic acid, a derivative of ferrocene, as electrochemical probe (Huang et al., 2009). In addition, ferrocene and its derivatives are also used as electron transfer mediators in all kinds of sensors owing to their reversible redox behavior of Ferrocene→Ferrocene$^+$ (Saleem et al., 2015; Xie et al., 2015; Ghosh et al., 2015).

Herein, we presented a highly sensitive non-enzymatic biosensor for the detection of H_2O_2 based on the multi-lays of platinum nanoparticles/reduced graphene oxide-chitosan-ferrocene carboxylic acid nano-hybrids (Pt NPs/RGO-CS-Fc nano-hybrids). Taking advantage of the high electrocatalytic efficiency of Pt NPs, high electronic conductivity of RGO and the reversible electrochemical behavior of Fc, the integration of different ingredients combined merits of each component and yielded enhanced properties via a synergistic effect. To the best of our knowledge, this is the first report on the application of Pt NPs/RGO-CS-Fc nano-hybrids for the construction of a non-enzymatic electrochemical H_2O_2 biosensor. This non-enzymatic biosensor was further used to detect the H_2O_2 concentrations released from different kinds of cells stimulated by extracellular matters and to evaluate the oxidative stress of different living cells.

2. Experimental

2.1 Reagents

Graphene oxide (GO) was purchased from Xianfeng Nano Materials Tech Co. Ltd. (Nanjing, China). ferrocene carboxylic acid (Fc), N-hydroxysulfosuccinimide sodium salt (Sulfo-NHS), N-(3-dimethylaminopropyl)-N-ethyl-carbodiimide hydrochloride (EDC), mercaptopropionic acid (MPA), $RuCl_3 \cdot XH_2O$, glutaraldehyde, $HAuCl_4 \cdot 4H_2O$, $H_2PtCl_6 \cdot 6H_2O$, $Pd(NO_3)_2 \cdot XH_2O$, chitosan (CS), ascorbic acid (AA), uric acid (UA) and β-D (+)-glucose were purchased from Sigma (St. Louis, MO, USA), Human hepatocarcinoma cell lines (HepG2), human normal liver cell (LO2) and human lung cancer cell line (A549) were purchased from the Chinese Academy of Medical Sciences (Beijing, China). All other reagents were of analytical grade and used without further purification. All solutions were prepared with ultra-pure water of 18 MΩ purified from a Milli-Q purification system (Milli-Pore, Bedford, MA, USA).

2.2 Instruments

The morphologies and surface structures were characterized with scanning electron microscope (SEM, Zeiss Ultra55, Germany) and transmission electron microscopy (TEM, JEM-2100, Japan). Raman spectra were measured on a DXR Raman microscope (Thermo Fisher Scientific, USA). The Fourier transform infrared (FT-IR) spectra were recorded on a FT-IR spectrometer (Bruker Tensor27, Germany) using KBr pellets.

All electrochemical measurements were performed on a CHI 660 electrochemical analyzer (Shanghai Chenhua Instrument Corporation, China) at room temperature. A conventional three-electrode system was used with modified gold electrode (GE) as the working electrode, saturated calomel electrode (SCE) as the reference electrode, and platinum (Pt) electrode as the auxiliary electrode. The electrochemical measurements were carried out in the electrolyte solution of phosphate buffer saline (PBS, pH 7.4, 0.02 M Na_2HPO_4/KH_2PO_4 and 0.1 M NaCl) and the electrolyte was bubbled with highly purity nitrogen for 15 min prior to use. Cyclic voltammetric (CV) was carried out in PBS containing 5 mM $K_3Fe(CN)_6/K_4Fe(CN)_6$ from -0.2 to 0.6 V with a 100 mV/s scanning rate or 1 mM H_2O_2 from -0.4 to 0.8 V with a 100 mV/s scanning rate. Electrochemical impedance spectroscopy (EIS) was carried out in PBS containing 5 mM $K_3Fe(CN)_6/K_4Fe(CN)_6$ at 0.24 V (versus SCE) with a frequency range of 0.1-100 kHz. All amperometric measurements were regularly carried out at -0.05 V in PBS with stirring.

2.3 Preparation of RGO-CS-Fc nona-hybrids

RGO was prepared according to the previous literation reports with minior modifications (Guo et al., 2011). Briefly, 30 μl hydrazine solution was added to 10 ml

GO suspension (0.5 mg/ml) and shaken for 10 minutes vigorously. Then the mixture was incubated in water bath at 60°C for 4 h. To isolate the RGO from the liquid, the mixed solution was centrifuged for 30 min at 20000 r.p.m. Following the removal of the supernatant, the black oily precipitate, that is RGO, was obtained and then washed twice with water. Finally, the RGO was re-dispersed in 5 ml water to form a 1 mg/ml solution and stored in refrigerator (4 °C) for future use.

RGO-CS-Fc nona-hybrids were prepared as the following proceed: 0.2 mg of chitosan into 10 ml acetic acid solution (1%) and stirred until no bubbles. 0.2 mg ferrocene acid，1 ml 10 mM EDC and 4 ml 10 mM sulfo-NHS solution were added and stirred four 4 h. When the color of the mixed solution changed from yellow to reddish brown, 0.2 ml 1 mg/ml RGO solution was added and then stirred for 24 h. After the mixed solution was centrifuged for 30 min at 20000 r.p.m, the supernatant was removed and the precipitates were washed twice. Finally, the precipitates were re-dispersed in 1 ml water and stored in refrigerator (4 °C) for future use.

2.4 Preparation of the Non-enzymatic Electrochemical biosensors based on the Pt NPs/RGO-CS-Fc nano-hybrids.

Gold electrode was polished sequentially with 0.3 and 0.05 mm Al_2O_3 powder, sonicated for 5 min each in ethanol and deionized water. 20 μl 10 μM of MPA was self-assembled on electrode in 4 °C overnight to obtain a functional electrode with carboxyl groups (-COOH). The electrode was washed twice with 0.02 M PBS, then the electrode was immersed in 10 mM EDC/NHS for 30 min in room temperature. After rinsed sufficiently with 0.02 M PBS, 20 μl RGO-CS-Fc solutions were dropped onto the modified GE and incubated for 30 min at 37 °C. In order to move away the un-adsorbed nano-hybrids, the electrodes were washed twice with 0.02 M PBS. Then the RGO-CS-Fc modified electrode was dipped into 10 mM H_2PtCl_6 solution and the

Pt NPs were electrodeposited on it by i-t curve at a constant potential of -0.2 V with a 100 mV/s scanning rate at room temperature with mild stirred. Subsequently, the modified electrode was cleaned carefully by doubly distilled water and soaked in the 2.5% glutaraldehyde (GA) solution for 15 min. After the electrode was washed with 0.02 M PBS, 20 μl RGO-CS-Fc suspensions were dropped on the electrode and incubated for 30 min at 37 °C and Pt NPs were electrodeposited again. These procedures were cycled for several times. Thus, a non-enzymatic electrochemical biosensor based on the Pt NPs/RGO-CS-Fc nano-hybrids (Pt NPs/RGO-CS-Fc biosensor) was come into being.

2.5 Exploration of the anti-interference capability of the Pt NPs/RGO-CS-Fc biosensor

In order to explore the anti-interference capability of the Pt NPs/RGO-CS-Fc biosensor, the amperometric responses at -0.05 V with the successive addition of 0.5 mM H_2O_2, 0.5 mM UA, 0.5 mM AA, 0.5 mM GLU, and a second 0.5 mM H_2O_2 into PBS were recorded.

2.6 Cell culture

The cell culture experiments were carried out using HepG2, LO2 and A549. They were cultured in RPMI-1640 medium containing 10% heat-inactivated fetal bovine serum, 100 μg/ml penicillin G and 100 μg/ml streptomycin at 37 °C in a humidified and 5% carbon dioxide atmosphere, and splitted every 2-3 days.

2.7 Detection of H_2O_2 in living cells with the Pt NPs/RGO-CS-Fc biosensor

Cells were collected by centrifugation for 5 min at 1000 r.p.m and washed twice with PBS. Cell number was calculated with cell counter. When the current decreased to a level less than 20 nA, AA was added into cells suspension to motivate cells to produce H_2O_2. The amperometric current response of H_2O_2 released from about 5.0 ×

10^6 cells was recorded by the Pt NPs/RGO-CS-Fc biosensor at -0.05 V (vs SCE) in 4 ml PBS.

3. Results and Discussion

3.1 Characterization of RGO-CS-Fc nano-hybrids

The as-prepared RGO-CS-Fc nano-hybrids were characterized with TEM, UV-vis, FT-IR and Raman spectra, etc. And the results were shown in Figure 1. Figure 1A depicts the TEM of RGO-CS-Fc nano-hybrids. It was clearly found that RGO exhibited a sheet structure and the sheet sizes were about 100 nm. The presence of RGO in the nano-hybrids was further confirmed by Raman spectrum, which showed in Figure 1B. It was clearly observed that there are two characteristic bands at 1353 cm^{-1} and 1596 cm^{-1}, representing the defects induced D band and the first-order scattering of the e_{2g} mode for the sp^2 carbon lattice (G band) (Sarkar et al. 2012), respectively, and the I_D/I_G intensity ratio was 0.99.

Figure 1C describes comparative FT-IR spectra of RGO (curve a), Fc (curve b), CS (curve c) and RGO-CS-Fc nano-hybrids (curve d). The RGO displayed clear characteristic peaks at 3439 cm^{-1} (stretching vibration of OH) and 1627 cm^{-1} (C=C stretching). In the FT-IR spectrum of Fc (curve b), the peaks at 3499 and 1392 cm^{-1} represent the stretching vibration of the OH and antisymmetric COO-, respectively, while the peak at 838 cm^{-1} is a characteristic of Fc ring. The peaks at 1599 and 1424 cm^{-1} (curve c) are attributed to N-H and C-N stretching, respectively. In the curve d, the peaks at 1530 and 1221 cm^{-1} can be attributed to N-H and C-O vibration, 816 cm^{-1} is indexed to Fc ring vibration. What's more, a new strong absorption peak ascribed to the CO-NH group can be observed clearly at 1711 cm^{-1}, implied that the amide interactions take place between -COOH and $-NH_2$ located at N atoms from CS and C

atoms from RGO and Fc. These results above suggested that the RGO-CS-Fc nano-hybrids were come into being. In addition, the UV-vis spectra of RGO, Fc and RGO-CS-Fc nano-hybrids shown in Figure 1D were also indicated that the RGO-CS-Fc nano-hybrids had been successfully synthesized.

In order to investigate the electrochemical properties of RGO-CS-Fc nano-hybrids, the nano-hybrids were immobilized on the surface of MPA-modified GE (MPA/GE) and the electrochemical signals were obtained by CV which using $[Fe(CN)_6]^{3-/4-}$ as electrochemical active probe (Figure 1E). A pair of reversible redox peak owing to the $[Fe(CN)_6]^{3-/4-}$ were exhibited on bare gold electrode (curve a), after MPA was immobilized on the GE, the redox current was declined and a non-reversible redox peak was obtained, which implied that the self-assembled film of MPA prevents the electron transfer between the $[Fe(CN)_6]^{3-/4-}$ and gold electrode (curve b). The reversible redox peak of $[Fe(CN)_6]^{3-/4-}$ can be regained when the RGO-CS-Fc nano-hybrids were modified on the surface of MPA/GE (curve c) and the current response was higher than the bare gold electrode. These results were illustrated that the RGO-CS-Fc nano-hybrids possessed excellent electron transfer ability. According to the Randled−Sevcik equation (Wang et al., 2015),

$$I_p=2.69\times10^5\ AD^{1/2}\ n^{3/2}\ \gamma^{1/2}\ C, \qquad (1)$$

where A represents the area of the electroactive surface area (cm^2), D represents the diffusion coefficient of the molecule in solution ($6.70 \pm 0.02 \times 10^{-6}$ $cm^2 \cdot s^{-1}$), n represents the number of electrons participating in the redox reaction (for $[Fe(CN)_6]^{3-/4-}$, n = 1), γ represents the scan rate of the potential perturbation ($V \cdot s^{-1}$), and C is the bulk concentration of the redox probe ($mol \cdot cm^{-3}$), the effective surface area of electrodes with various modifications were calculated in the trend of MPA/GE

($0.0154\ cm^2$) < bare GE ($0.0178\ cm^2$) < RGO-CS-Fc/GE ($0.0214\ cm^2$), indicating that RGO-CS-Fc nano-hybrids can enlarge the effective surface area of electrodes.

(Figure 1 insert here)

1.2 Analytical principle of the non-enzymatic electrochemical biosensor based on Pt NPs/RGO-CS-Fc nano-hybrids

In this work, a non-enzymatic H_2O_2 sensor based on Pt NPs/RGO-CS-Fc Nano-hybrids was fabricated and the analytical principle is schematically illustrated in Scheme 1. First, the RGO-CS-Fc nano-hybrids were synthesized by the conjugate of the amino ($-NH_2$) in CS with the carboxyl (-COOH) in RGO and Fc using EDC/NHS method. Then, the RGO-CS-Fc nano-hybrids were immobilized onto the gold electrode modified with the self-assembly of MPA. After that, Pt NPs were electro-deposed onto the RGO-CS-Fc nano-hybrids modified gold electrode. After the procedures were cycled in turn for several times, a Non-enzymatic Electrochemical Biosensor, Pt NPs/RGO-CS-Fc biosensor, was come into being. Among the multilayer of Pt NPs/RGO-CS-Fc nano-hybrids, Fc molecules, acting as electron mediators, were integrated into the sensor by grafting on chitosan. While RGO was acted as the enhanced materials to increase the electrical conductivity of the bio-composite film and promote electron transfer of the incorporated electroactive Fc mediators, improving the sensitivity of the prepared biosensor. Hence, when the H_2O_2 was disintegrated with the catalysis of Pt NPs, the electrons produced in this reaction could be transferred quickly to the gold electrode and produced a sensitive current for the quantification of H_2O_2. Thus, the Pt NPs/RGO-CS-Fc biosensor can be readily

applied for the detection of the H_2O_2 released from the living cells during the redox homeostasis disrupted by ascorbic acid.

(Scheme 1 insert here)

3.3 Electrochemical behaviors of the Pt NPs/RGO-CS-Fc biosensor

Figure 2A shows the CV and amperometric current response for the bare gold electrode (bare GE), MPA-modified gold electrode (MPA/GE), and the Pt NPs/RGO-CS-Fc biosensor with 1, 2, 3, 4, 5, 6 layers of Pt NPs/RGO-CS-Fc nano-hybrids, respectively. As shown in Figure 2A, an reduction peak of H_2O_2 emerges in the presence of 0.1 mM H_2O_2 in PBS, and the increasing of the layers of Pt NPs/RGO-CS-Fc nano-hybrids can increase the reduction peak current of H_2O_2 (curve c→h). As a control, a negligible reduction peak of H_2O_2 can be obtained on bare GE (curve a) or MPA/GE (curve b).

Amperometric current response was used to the quantification of H_2O_2 with the Pt NPs/RGO-CS-Fc/GE biosensor. Figure 2B exhibits the response of Pt NPs/RGO-CS-Fc nano-hybrids modified-GE for the detection of 1 mM H_2O_2 in PBS at -0.05 V. When H_2O_2 was added in PBS, it is evident that Pt NPs/RGO-CS-Fc nano-hybrids modified-GE exhibited enhanced amperometric response for H_2O_2 detection (curve f) compared with the other controls with different modifications, including bare GE (curve a), RGO-CS-Fc/GE (curve b), Pt-GE (curve c), Fc-CS/Pt/GE (curve d) and Pt/RGO-CS/GE (curve e), respectively. The steady-state current of Pt NPs/RGO-CS-Fc nano-hybrids modified-GE could stable within 2 s after the injection of H_2O_2. Especially, no clear response or only weak signal was obtained on the bare GE and RGO-CS-Fc/GE, respectively, implied that the presence of Pt NPs

is necessary for the produce of reduction current of H_2O_2. Moreover, the inset in Figure 2B shows the bar graphs of amperometric current response with different modification electrodes.

EIS, a valid method for exploring the properties of surface modified electrodes, was performed to further explore the different modification stages that occur on the electrode surface and the results were shown in Figure 2C. EIS of bare GE displayed low Ret (charge-transfer resistance) of 230 Ω (curve a). After the MPA was self-assembled on the gold electrode surface, the resistance was increased to 1000 Ω because of its non-conductivity (curve b). When RGO-CS-Fc nano-hybrids were modified on the electrode and Pt NPs were electrodeposited onto the surface of RGO-CS-Fc nano-hybrids film, the resistance decreased to 190 Ω (curve c), implying that the composite of RGO-CS-Fc film and Pt NPs possess a good electric conducting properties. However, along with the increase of the layers of Pt NPs/RGO-CS-Fc nano-hybrids film, the resistance was increased to 1630 Ω (curve d, 4 layers), 3150 Ω (curve e, 5 layers), 10000 Ω (curve f, 6 layers), respectively, which indicating that the formation of the multilayers of Pt NPs/RGO-CS-Fc nano-hybrids film increase charge transfer resistance of $K_3Fe(CN)_6/K_4Fe(CN)_6$ on the electrode surface.

(Figure 2 insert here)

3.4 Characterization of the Pt NPs/RGO-CS-Fc biosensor

The SEM images demonstrate the morphology of electrodes modified with various materials. One can see clearly from Figure 3A that the bare GE gives a uniform dark image, while there are some bright spots randomly distributed in the image of the Pt NPs/RGO-CS-Fc nano-hybrids modified-GE (Figure 3B). This

implied that the Pt NPs had been successfully generated with an electrodeposition procedure on gold electrode. According to the SEM image, it could be estimated that the Pt NPs modified on GE had a diameter of approximately 200 nm on the average. Figure 3C depicts Raman spectra of RGO-CS, RGO-CS-Fc and Pt NPs/RGO-CS-Fc nano-hybrids on the surface of gold electrode. A pair of peaks can be seen obviously at 1352 cm^{-1} (D-band) and 1591 cm^{-1} (G-band) , however, the intensity of D-band and G-band of Pt NPs/RGO-CS-Fc nano-hybrids (curve c) was lower than that of RGO-CS (curve a) or RGO-CS-Fc (curve b). All these results suggested that the Pt NPs/RGO-CS-Fc nano-hybrids were modified on gold electrode and the Pt NPs/RGO-CS-Fc biosensor was successfully formed.

(Figure 3 insert here)

3.5 Optimization of the determining conditions.

The performance of Pt NPs/RGO-CS-Fc biosensor for the reduction of H_2O_2 was optimized by varying different metallic catalysts, electrodeposition time of Pt NPs and different layer of Pt NPs/RGO-CS-Fc nano-hybrids film. Figure 4A depicts the behavior of the sensor with the different metallic catalysts (Au, Pd, Pt and Rh). As shown in Figure 4A, the highest response current of H_2O_2 obtained by using Pt as catalyst is about 22, 56, 198 times as high as that by using Ru, Pd or Au as catalyst, respectively. This result demonstrated that Pt catalyst show obvious improvement in activity compared with other metallic catalysts.

Figure 4B shows the response currents of H_2O_2 with the different layer of Pt NPs/RGO-CS-Fc nano-hybrids film on the modified electrode. It is clearly seen that the current response increased gradually as the layers of Pt NPs/RGO-CS-Fc

nano-hybrids film increased from 1 to 5, and when the layer of Pt NPs/RGO-CS-Fc nano-hybrids film reached six, the current response did not further increased. Thus, six layers of Pt NPs/RGO-CS-Fc nano-hybrids film were chosen for further experiments.

Figure 4C depicts the effect of electrodeposition time of Pt NPs on the electrocatalytic reduction of H_2O_2. The current response increased as the deposition time increased from 10 to 90 s and reached the maximum value at 90 s. Then the current response decreased with the further prolonged deposition time. Hence, the deposition time of 90 s was selected to the further experiments.

(Figure 4 insert here)

3.6 Performance of Pt NPs/RGO-CS-Fc biosensor toward H_2O_2

Here we use the RGO-CS-Fc nano-hybrids and Pt NPs as a synergistic catalyst to facilitate the reduction of H_2O_2 and measure the reduction current at a certain potential. Under the optimum experimental conditions discussed above, *i-t* curve was used for determination of H_2O_2. Figure 5A displayed the current response of the Pt NPs/RGO-CS-Fc biosensor for the successive addition of H_2O_2 with different concentrations in 0.02 M PBS (pH 7.0). According to the Figure 5A, the current response presented a linear relationship with H_2O_2 concentration from 2.0×10^{-8} M to 3.0×10^{-6} M with a correlation coefficient of R^2=0.9968 and with logarithm of H_2O_2 concentration from 6.0×10^{-6} M to 1.0×10^{-2} M with a correlation coefficient of R^2=0.9887 (inset in Figure 5A). The low detection limit of 20 nM at the signal/noise(S/N) ratio of 3. The sensing performance of the developed biosensor for detection of H_2O_2 was compared with the previous reports and shown in Table 1.

Based on the comparison listed in Table 1, the Pt NPs/RGO-CS-Fc biosensor possessed better performances with the lowest detection limit for the detection of H_2O_2.

The anti-interference ability is a major challenge in biosensor, the influence of electrochemical response signals species were studied for their interference with the amperometric response of H_2O_2. Under the optimal conditions, the interference experiments were investigated by comparing the response current of 0.5 mM of H_2O_2 plus three relevant electroactive species (0.5 mM AA, 0.5 mM UA, 0.5 mM GLU) with that of 0.5 mM of H_2O_2 alone. The results (Figure 5B) showed that negligible response to the injection of interfering species at their physiological concentration level, which indicate that AA, UA and GLU have no interference in the detection of H_2O_2.

To study the reproducibility of the non-enzymatic sensor, six Pt NPs/RGO-CS-Fc biosensors were prepared by the same method and tested for the H_2O_2 under the same condition. The RSD was 7.0% at 1 mM of H_2O_2, showing an acceptable reproducibility.

The Pt NPs/RGO-CS-Fc biosensors were stored in a humid environment at 4°C when the sensors were out of use. The Long-term stability of the biosensor was evaluated by measuring the current response to 1 mM H_2O_2 once a day. The current response was 80% of the original value after 22 days.

(Figure 5 insert here)

(Table 1 insert here)

3.7 Measurements of H_2O_2 release from living cells.

To explore the application of the Pt NPs/RGO-CS-Fc biosensor, the detection of H_2O_2 in living cells was performed. Figure 6A showed the amperometric responses curve of the Pt NPs/RGO-CS-Fc biosensor in the presence of HepG2 cells irritated by AA in physiological PBS (Figure 6A, curve c). While the cells with HRP and the PBS as the control groups under the same conditions had no current change (Figure 6A, curve a, b). When injection of AA, the response current caused in HepG2 cells was increased obviously. However, the cells with HRP and the PBS as the control groups under the same conditions had no current change.

Measurement of H_2O_2 is significant for assess of living cell oxidative stress and distinctions of capability oxidative stress in different living cells. So, we detected current of H_2O_2 released by the same certain amount of A549, HepG2 and L02 cell lines stimulated by 1 μM AA and the result showed in Figure 6B. Seen from Figure 6B, the tumor cells (A549, HepG2) generated more H_2O_2 than normal cell lines (L02), which indicated that abnormal growth of the tumor have an enhancement of ROS production ability, and it is meaningful for investigate of the environment in tumor cells and the therapy of cancer. Also, the optical morphology of cells (L02, A549, HepG2) before and after the addition of AA were shown in Figure 6C. The optical microscopy during the measurements showed that all the cells kept their regular shapes and there were no difference before and after the addition of AA. But the concentration of H_2O_2 in tumor cells keeps a higher value than in normal cells. These results demonstrate that the non-enzymatic biosensor can be used for detection of H_2O_2 release from cells and could be potentially useful for physiological and pathological studies.

(Figure 6 insert here)

4. Conclusions

In summary, we have designed a non-enzymatic electrochemical H_2O_2 biosensor based on the multi-layer of Pt NPs/RGO-CS-Fc nano-hybrids, which were obtained through electrochemical deposition Pt NPs on the surface of the RGO-CS-Fc nano-hybrids. Based on the excellent biological compatibility and electron transfer ability of RGO-CS-Fc nano-hybrids and the excellent electrochemical catalysis properties of Pt NPs, the Pt NPs/RGO-CS-Fc biosensor showed a dynamic response in linear dependency upon the logarithm of H_2O_2 concentration through a four-decade concentration range from 6.0×10^{-6} M to 1.0×10^{-2} M, and upon the H_2O_2 concentration through a two-decade concentration range from 2.0×10^{-8} M to 3.0×10^{-6} M with a readily achievable detection limit of 20 nM. Besides, this sensor showed an outstanding anti-interference ability, acceptable reproducibility and stability. This biosensor has displayed great possibility applications in the measurement of H_2O_2 released from the living cells, which is meaningful for evaluate oxidative stress of different kinds of cancer cells in the clinical diagnostics.

Acknowledgments

This work is supported by the National Natural Science Foundation of China (Nos. 21265003, 81406451), Program for New Century Excellent Talents in University of Chinese Ministry of Education (NCET-13-0744), the Postdoctoral research fund of China (No. 2013T60830), Fund of Guangxi Key laboratory of Metabolic Diseases Research (No. 2015-181h-02, 2015-181h-03), Innovation Project of Guangxi Graduate Education (No. YCSZ2015151) and Project of outstanding young teachers' training in higher education institutions of Guangxi.

Reference

Bianchi, R.C., Silva, E.R., Antonia, L.H., Ferreira, F.F., Alves W.A., 2014. Langmuir 30, 11464−73.

Borgmann, S., 2009. Anal. Bioanal. Chem. 394, 95−105.

Chakraborty, S., Raj, C. R., 2009. Biosens. Bioelectron. 24, 3264−3268.

Chakrapani, H., 2014. ACS Med. Chem. Lett. 5, 777−781.

Chang, H., Wang, X., Shiu, K.-K., Zhu, Y., Wang, J., Li, Q., Chen, B., Jiang, H., 2013. Biosens. Bioelectron. 41, 789−794.

Chen, H.F., Wang, X.P., Liu, G.T., Lin, A.J., Wen, Y., Yang, H.F., 2015. Sci China Chem. 58, 1585-1592.

Chen, S., Hai. X., Chen, X.W., Wang, J.H., 2014. Anal. Chem. 186 (13), 6689-6694.

Chen, X.M., Lin, Z.J., Chen, D.J., Jia, T.T., Cai, Z.M., Wang, X.R., 2010. Biosens. Bioelectron. 25, 1803-1808.

Dey, R.S., Raj, C. R., 2010. J. Phys. Chem. C 114 (49), 21427–21433.

Ghosh, T., Sarkar, P., Turner, A.P., 2015. Bioelectrochemistry 102, 1-9.

Gimeno, P., Bousquet, C., Lassu, N., Maggio, A. F., Civade, C., Brenier, C., Lempereur, L. J., 2015. Pharm. Biomed. Anal. 107, 386−393.

Han,T.T., Zhang, Y., Xu J.Q., Dong, J.P., Liu C.C., 2015. Sens. Actuators B 207, 404–412.

Huang, Y., Zhang, Y.L., Xu, X., Jiang, J.H., Shen, G.L., Yu, R.Q., 2009. J. Am. Chem. Soc. 131(7), 2478–2480.

Khodade, V.S., Sharath, C.M., Banerjee, A., Lahiri, S., Pulipeta, M., Rangarajan, R., Lee, Y.J., Park, J.Y., 2010. Biosens. Bioelectron. 26, 1353-1358.

Li, J., Li, Y., Zhang, Y., Wei, G., 2012. Anal. Chem. 84, 1888−1893.

Lin, L., Song, X., Chen, Y., Rong, M., Zhao, T., Wang, Y., Jiang, Y., Chen, X., 2015. Anal. Chim. Acta. 15, 869, 89-95.

Lu, P., Yu, J., Lei, Y.T., Lu, S.J., Wang, C.H., Liu, D.X., 2015. Sensor. Actuat. B-Chem. 208, 90-98.

Luo, Y.P., Liu, H.Q., Rui, Q., Tian, Y., 2009. Anal. Chem. 81, 3035–3041.

Ma, M., Miao, Z., Zhang, D., Du, X., Zhang, Y., Zhang, C., Lin, J., Chen, Q., 2015. Biosens. Bioelectron. 15, 64, 477-484.

Qin, X., Wang, H.C., Miao, Z.Y., Li, J.L., Chen, Q., 2015.Talanta 139, 56-61.

Qiu, J.D., Huang, J., Liang, R.P., 2011. Sens. Actuators B 160, 287-294.

Sahin, O.G., 2015. Electrochim Acta.180, 873-878.

Saleem, M., Yu, H., Wang, L., Khalid, H., Akram, M., Abbasi, N.M., Huang, J., 2015. Anal. Chim. Acta. 30, 876, 9-25.

Sarkar, S., Bekyarova, E., Haddon, R.C., 2012. Angew. Chem. Int. Ed. 51, 4901 – 4904

Shen, W.J., Zhuo Y., Chai, Y.Q., Yang, Z.H., Han, J., Yuan, R., 2015. ACS. Appl. Mater. Inter. 7, 4127−4134.

Shi, Y., Su, P., Wang, Y., Yang, Y., 2014. Talanta 130, 259-264.

Wang, L., Zhang, Y., Cheng, C., Liu, X., Jiang, H., Wang, X., 2015. ACS. Appl. Mater. Inter. 7, 18441-18449.

Wen, F., Dong, Y., Feng, L., Wang, S., Zhang, S., Zhang, X., 2011. Anal. Chem. 83,1193−1196.

Wu, P., Cai, Z., Gao, Y., Zhang, H., Cai, C., 2011. Chem. Commun. 47, 11327-11329.

Xie, S., Zhang, J., Yuan, Y., Chai, Y., Yuan, R., 2015. Chem. Commun. 25, 51(16), 3387-3390.

Xiong, L.Y., Zheng, L.Z., Xu, J.P., Liu, W., Kang, X.W., Wang, W., 2014. Ecs Electrochem Lett. 3, B26-B29.

Yu, D., Wang, P., Zhao, Y., Fan, A., 2016. Talanta 146, 655-661.

Yu, G.X., Wu W.X., Pan, X.Q., Zhao, Q., Wei, X.Y., Lu, Q., 2015. Sensors 15, 2709-2722.

Zhang, J., Ma, J.L., Zhang, S.B., Wang, W.C., Chen, Z.D., 2015. Sensor. Actuat. B-Chem. 211, 385-391.

Zhang, Y., Wu, C., Zhou, X., Wu, X., Yang, Y., Wu, H., 2013. Nanoscale 5, 1816-1819

Zhang, Y.Y., Bai, X.Y., Wang, X.M., Shiu, K.-K., Zhu, Y.L., Jiang, H., 2014. Anal. Chem. 86, 9459−9465.

Table 1 Comparison of analytical performance with some other biosensors for detection of hydrogen peroxide

Electrode material	Linear range (mM)	Sensitivity (μA/mM)	LOD(μM)	Reference
Ag NWs	0.006–10	0.785	2	Qin et al. 2015
ERGO-Ag	0.0016–9	–	1.6	Zhan et al. 2015
Ag-MWCNTs	0.05–17	1.42	0.5	Zhan et al. 2009
Bimetallic Nanocrystals	–	195.3	8.4	Han et al. 2015

Pt NPs-GO	–	341.14	0.5	Zhang et al. 2015
RGO/$AuFe_3O_4$/Pt	0.005–11.5	–	0.1	Wang et al. 2015
Pt/RGO-CS-Fc	0.00002-0.003	–	0.02	this work
	0.006-10			

Figure Captions

Scheme 1 Analytical principle for the detecting of H_2O_2 in living cells with the non-enzymatic biosensor based on Pt NPs/RGO-CS-Fc nano-hybrids.

Figure 1 Characterization of RGO-CS-Fc nano-hybrids. (A) TEM of RGO-CS-Fc nano-hybrids, (B) Raman spectrum of RGO-CS-Fc nano-hybrids, (C) FT-IR of (a) RGO, (b) Fc, (c) CS, (d) RGO-CS-Fc nano-hybrids, (D) UV-vis spectra of (a) RGO, (b) Fc, (c) RGO-CS-Fc nano-hybrids, (E) Cyclic voltammogram response of various electrode: (a) bare GE, (b) MPA/GE, (c) RGO-CS-Fc/MPA/GE from -0.2 to 0.6 V (versus SCE) with a scan rate of 100 mV/s in PBS containing 5 mM $[Fe(CN)_6]^{3-/4-}$.

Figure 2 Electrochemical behaviors of the Pt NPs/RGO-CS-Fc biosensor. (A) CV response of (a) bare GE, (b) MPA/GE, (c, d, e, f, g, h) 1, 2, 3, 4, 5, 6 layers of Pt NPs/RGO-CS-Fc nano-hybrids on the surface of MPA/GE in the presence of 0.1 mM H_2O_2 in PBS from -0.4 to 0.8V with a 100 mV/s scanning rate. (B) Amperometric current response toward 1 mM H_2O_2 at -0.05 V in 0.02 M PBS with different modification electrode: (a) Bare GE, (b) RGO-CS-Fc/GE, (c) Pt NPs/GE, Fc-CS/Pt NPs/GE (d) and Pt NPs/RGO-CS/GE (e) Pt NPs/RGO-CS-Fc/GE (f). (Inset shows the bar graphs of amperometric current response with different modification electrodes.

Error bars represent the standard error of the mean (n=3 electrodes)). (C) EIS of bare GE (a), MPA/GE (b), Pt NPs/RGO-CS-Fc/GE (1 cycle) (c), Pt NPs/RGO-CS-Fc/GE (4 cycle) (d), Pt NPs/RGO-CS-Fc/GE (5 cycle) (e), Pt/RGO-Fc-CS/GE (6 cycle) (f) in PBS containing 5 mM $Fe(CN)_6^{3-/4-}$ at 0.24 V (versus SCE) with a frequency range of 0.1-100 kHz.

Figure 3 Characterization of the Pt NPs/RGO-CS-Fc biosensor. SEM images of (A) bare electrode and (B) Pt NPs/RGO-CS-Fc nano-hybrids. (C) Raman spectra of (a) RGO-CS, (b) RGO-CS-Fc and (c) Pt NPs/RGO-CS-Fc.

Figure 4 (A) Catalyze capability of different kinds of metal nanoparticles toward the H_2O_2. (B) Optimization of the layer of Pt NPs/RGO-CS-Fc nano-hybrids film on the GE. (C) Electrodeposition time of Pt NPs on the modified electrode. Error bars are the standard error of the mean (n=3 electrodes).

Figure 5 (A) Amperometric current response of the Pt NPs/RGO-CS-Fc biosensor at -0.05 V with successive addition of H_2O_2 in 0.02 M PBS ranging from 2.0×10^{-8} to 1.0×10^{-2} M and Linear relation (inset). (B) Amperometric current response of the Pt NPs/RGO-CS-Fc biosensor at -0.05 V with successive addition of 0.5 mM H_2O_2, 0.5 mM AA, 0.5 mM UA, 0.5 mM GLU and a second 0.5 mM H_2O_2 in 0.02 M PBS. Error bars are the standard error of the mean (n=3 electrodes).

Figure 6 (A) Time course of the H_2O_2 release from HepG2 cells upon the addition of 1 μM AA. Curve a is for the experiment HepG2 cells and catalases; Curve b is for the experiment without cells. Curve c is for the experiment HepG2 cells. (B)

Amperometric current response of the Pt NPs/RGO-CS-Fc biosensor at -0.05 V to H_2O_2 released by A549, HepG2 and L02 cell lines stimulated by 1 μM AA. (C) the optical morphology of cells (L02, A549, HepG2) before and after the addition of AA. Error bars are the standard error of the mean (n=3 electrodes). *P<0.05, ***P<0.001.

Highlights

- A highly sensitive non-enzymatic electrochemical sensor based on Pt NPs/RGO-CS-Fc nano-hybrids was developed.
- This biosensor integrated the high electrocatalytic efficiency of Pt NPs, high electronic conductivity of RGO and the reversible electrochemical behavior of Fc and yielded enhanced properties via a synergistic effect.
- The non-enzymatic electrochemical biosensor exhibited excellent anti-interference capability and reproducibility for the detection of H_2O_2.
- The non-enzymatic electrochemical biosensor was also successfully applied for the detection of H_2O_2 from living cells.